Challenges with onboard strain measurements on a model Francis turbine runner

Journal of Physics: Conference Series **2629** (2023) 012004 doi:10.1088/1742-6596/2629/1/012004

Challenges with onboard strain measurements on a model Francis turbine runner

Johannes Kverno[1]*, Gaute Elde Vefring[1], Igor Iliev[2], Bjørn Winther Solemslie[3] and Ole Gunnar Dahlhaug[1]

[1] Department of Energy and Process Engineering, Norwegian University of Science and Technology, Alfred Getz' vei 4, 7034 Trondheim, Norway
[2] SINTEF Energi AS, Sem Sælands vei 11, 7034 Trondheim, Norway
[3] Departement of of Aquatic Biodiversity, Norwegian Institute for Nature Research, Høgskoleringen 9, 7034 Trondheim, Norway

* E-mail: johannes.kverno@ntnu.no

Abstract. As the world transitions towards more renewable energy sources, as a step to reduce the emissions of CO_2, intermittent and non-dispatchable sources like solar and wind will take up a larger proportion of the energy production. With more unregulated power in the energy mix, a higher demand is put on the rest of the energy production system. Hydropower is in a unique position as it is both renewable and a highly flexible energy source. The increased use of flexible operation of Francis turbines especially, puts a higher dynamic load on the runner components which as a consequence leads to a reduced lifetime. In this paper we present the experimental setup and results from a measurement campaign performed on a model of a low specific speed Francis runner. Onboard measurements with strain gauges at the trailing edge of two runner blades were performed. The experiments were conducted as a part of the HydroFlex project with the goal of validating numerical simulations and to gain a better understanding of the reduction of lifetime on Francis turbines due to higher fatigue loading from more flexible operation. The results shows that there were a significant drift of the mean strain over time during the measurement campaign, and a lower measured strain at BEP than expected when compared to numerical simulations. In this paper, the experimental setup, results and challenges encountered are presented.

1. Introduction

The European Union, and most other countries in the world, have committed to reduce the emission of CO_2 and cut down on the reliance on fossil fuels. Within the EU, this means that at least 32% of the electrical energy production must come from renewable sources by 2030 [1] and by 80% by 2050 [2]. Two of the major renewable energy sources is wind and solar, both of which are intermittent sources. Since the electrical grid must be balanced between production and consumption, the introduction of a large fraction of non-dispatchable energy sources to the grid mix can lead to instabilities and damage to connected components if no other action is taken. As a consequence, the remaining energy producers on the grid must adjust their power output more frequently to keep the grid stable, both as demand changes and as there are changes in the incoming energy from the intermittent sources. Hydropower in Europe is in a unique position being a well developed, highly flexible and renewable energy source. The most commonly used type of turbine in hydropower is the Francis turbine and the

mean age of the large Francis turbines are around 50 years. They were originally designed for very steady operation pattern with relatively little changes in the load. Future operation of the turbines will require high flexibility, leading to more fatigue and damage to the units. The runner is the most vulnerable part of the Francis turbine. This paper is about fatigue loads in the runner blades of Francis turbines. In order to gain a better understanding of how the blades of a Francis turbine is loaded during start-stop, ramping and off-design conditions a set of strain gauges were mounted at the trailing edge of two neighbouring blades. The location of the strain gauges were selected to be as close as possible to the "hot spots" where the maximum static principal strains occur. Additionally, because the strain gauge provides an averaged value of the strain over the area of the strain gauge itself, and not at a single point, locations with large gradients should be avoided. For this purpose, fluid-structure interaction simulations were initially performed at several operating points within the HydroFlex project. According to the simulations, the location of the hot spots remains nearly fixed throughout the entire operating range of the turbine, and the expected dynamic stresses are relatively low in comparison to the static stresses for the tested head. The trailing edge is typically also where cracks and material failure tend to appear in prototype runners. A model turbine has been set up at the Waterpower laboratory.

2. Experimental setup

2.1. Test rig and turbine runner

The experiments were done on a Francis model test rig at the Waterpower laboratory, NTNU, with a setup compliant with the IEC 60193 standard [3]. The test rig is a low specific speed Francis model turbine with a runner outlet diameter of $0,349$m and a maximum rated head of 30m. The spiral casing consists of 14 stay vanes and 28 guide vanes, while the turbine runner is made up of 17 blades. An 8 pole 3-phase 315kW asynchronous generator is connected to the turbine shaft and is used to control and maintain the rotational speed. Control and measurement of the test rig is handled by a National Instruments compactRIO and LabVIEW system. The turbine runner used for the experiments is the Francis-101 (F101) which was tailor made for the HydroFlex project [4] and the experiment itself. The runner blade design was optimised for onboard measurements to compare and validate numerical simulations with the experimental results as the key objective. The runner dimensions were also constrained by the existing spiral casing and covers which are a scaled down model of the Tokke Power Plant [5], and it has the same external dimensions as the Francis-99 (F99) research turbine [6]. Another important design criteria was to maintain a similar efficiency characteristic as the F99 runner and with the best efficiency point (BEP) being at the same point of operation. While the leading edge (LE) of the blades were optimised solely with the hydraulics in mind, the trailing edge (TE) were not. The TE were made as thin as possible to increase the response of the strain measurements and with a radial edge [7]. The entire length of the runner blades also had to be firmly fixed within the blade sections (illustrated in Figure 1). It was important to have control over the contact surfaces and friction between the blade sections and the hub disk and shroud cover, so no unattached blade sections extends beyond the blade section. The runner is also designed on the same platform as the Francis-100 (F100) runner developed in the HydroCen research project [8, 9] at the Waterpower Laboratory. So while F-101 shares the same hub disk and shroud cover with the F100 runner, the blades can be designed with a lot of freedom since the hydraulic surfaces of the hub and shroud also is a part of the blade sections. The design itself was made with the same quadratic surface model as the F100, but with 12 free parameters instead of the original 15 [7]. With the design of the runner assembly, relatively little space was left for instrumentation on board, with the only dry location with room for electronics being within the center bushing, as seen in Figure 1. This packing constraint limited the number of onboard sensors and amplifiers that could be fitted.

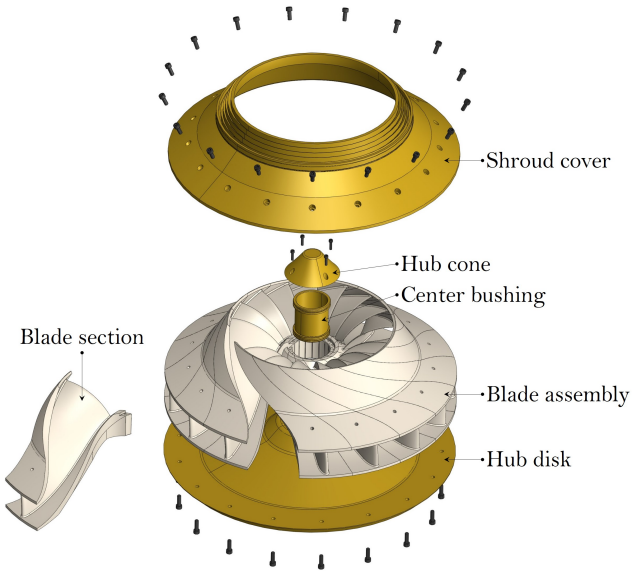

Figure 1: Exploded view of the F101 runner used for the experiments showing its method of assembly.

2.2. Experiment setup

The test rig includes a whole suite of sensors to measure flow rate, pressures, rotational speed, level of dissolved oxygen in the water, shaft bearing friction torque, etc. In addition, pressure sensors were mounted on the rig, two on the draft tube cone near the outlet of the runner separated by 180°, and three on the top cover in the vaneless space between the guide vanes and runner inlet. On board the runner there were two pairs of strain gauges mounted on the suction side of the TE near the hub and shroud, on two neighbouring blades. The transmission of the data and power supply from the rotating to stationary domain was through sliprings mounted on the turbine shaft. Sliprings were chosen to avoid the issue of data synchronisation when having two individual and separated sets of measurement chains. In order to minimise the noise to signal ratio, amplification of the sensor output were done onboard as well. After the slipring the signal were fed into a DAQ module placed near the rig, also illustrated in Figure 2.

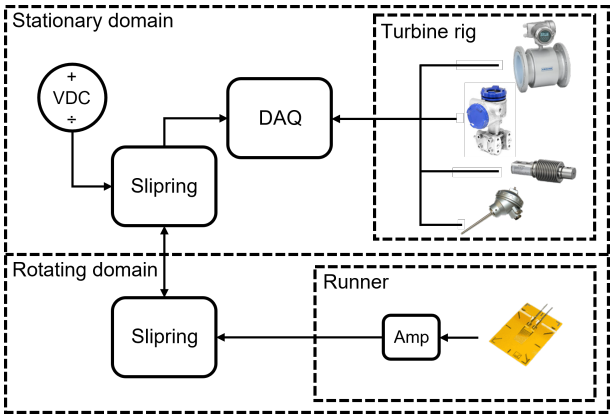

Figure 2: Illustration of the measurement chain as used in the experiments

2.3. Sensors and calibration

The strain gauges chosen for the experiment was the 1-LY41-6/350 1 grid linear strain gauge by HBM [10]. This choice was made due to its relatively small grid size and similar thermal expansion properties as the runner blade material itself. The exact positioning was chosen based on numerical simulations of where the strain gradients would be as low as possible, but still with a high enough strain to capture it to minimise the uncertainty. The direction of the strain gauges were parallel to the TE, which is in line with the direction of the maximum principal static strains. Since the strain gauges were single grid gauges the rest of the Wheatsone bridge was completed in the hub next to the amplifiers with three high precision 350Ω metal foil resistors [11]. One goal of this measurement campaign was to get a better understanding of the actual stress in the blades at the location of the strain gauges. In order to enable the validation of the numerical simulations that were performed on the same turbine runner. To get the stress from the measured strain, a calibration rig and procedure was developed where a series of loads would be applied to the blade and the response and amplified output from the chain was recorded. Then, the same set of loads were set up in a numerical simulation and the material stress in the same location and direction as the strain gauges were stored, giving a calibration from measured volts to strain. More details and results of the strain gauge calibration will be the topic of another upcoming publication. The calibration of the rest of the sensors attached on the Francis test rig were performed in compliance with the IEC60193 standard [3].

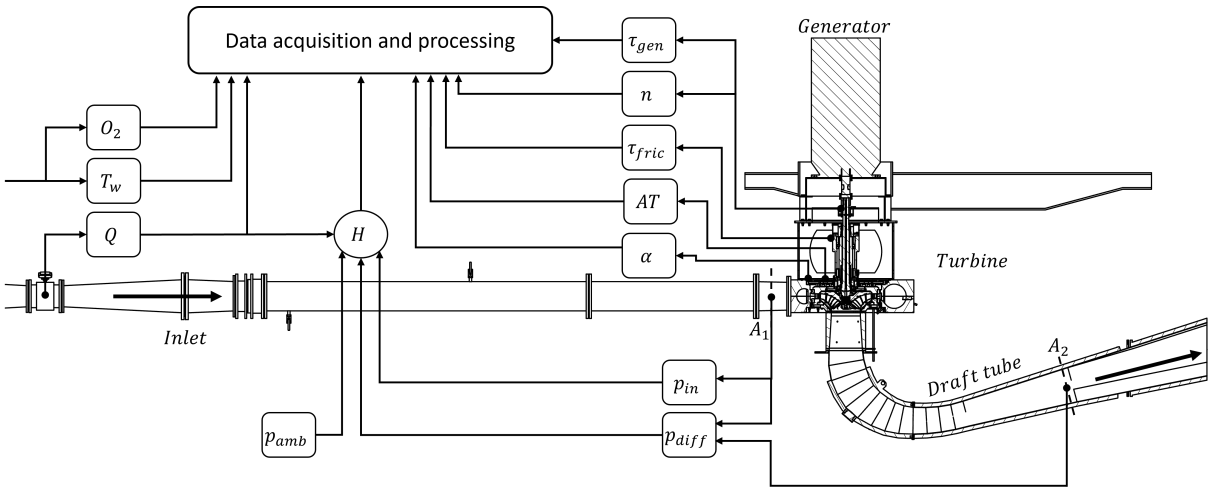

Figure 3: Overview of the test rig and the location of the measurements.

2.4. Signal conditioning and acquisition

The selected amplifiers were Mantracourt ICA3H embedded strain gauge analouge amplifiers [12]. The ICA3H uses a bipolar DC power supply of ±14V with a bridge excitation voltage of 5V and an output of ±10V. The amplifier gain had to be increased from the default factory configuration in order to get a large enough signal response from an applied load on the blade. In the end, it was decided that a 1026× gain was the best compromise, with a signal response in the 10^0V order of magnitude and still small enough to allow some temperature related drift without clipping the signal.

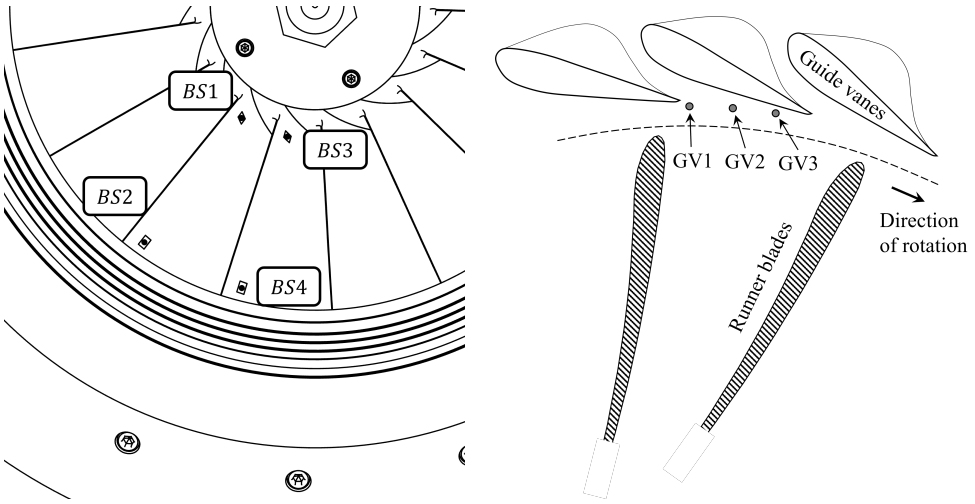

(a) Outlet of turbine runner

(b) Vaneless space between the wicket gate and turbine runner

Figure 4: Detailed view of the location of strain gauges (a) and pressure sensors (b) mounted on the turbine test rig

Measurand	Symbol	Unit	Manufacturer	Uncertainty	Sampling rate
Flow rate	Q	[m^3/s]	Krohne	$\pm 0,128\%$	10Hz
Inlet	p_{in}	[kPa]	GE Druck	$0,059$kPa	5000Hz
Differential	p_{diff}	[kPa]	Fuji	$0,066$kPa	5000Hz
Ambient	p_{amb}	[kPa]	Vaisala	$\pm 0,025$kPa	1Hz
Vaneless space	$GV\#$	[kPa]	Kulite	$0,29$kPa	5000Hz
DT pressure	$DT\#$	[kPa]	Kulite	$0,030$kPa	5000Hz
Blade strain	$BS1$	[μm/m]	HBM	$1,2307\mu$m/m	5000Hz
	$BS2$	[μm/m]	HBM	$0,9971\mu$m/m	5000Hz
	$BS3$	[μm/m]	HBM	$1,2641\mu$m/m	5000Hz
	$BS4$	[μm/m]	HBM	$0,7639\mu$m/m	5000Hz
Water temp.	T_w	[°C]	Siemens	$\pm 0,005\%$	10Hz
Shaft torque	τ_{gen}	[Nm]	HBM	$0,003\%M_{Nom}$	50Hz
Friction torque	τ_{fric}	[Nm]	Hottinger	$0,83$Nm	5000Hz
Speed of rotation	n	[RPM]	HBM	$\pm 1,5$RPM	50Hz
Axial thrust	AT	[kN]	Fuji	$\pm 0,1\%Fs$	5000Hz
Guide vane angle	α	[°]	Stegmann	$\pm 0,05°$	1Hz
Dissolved oxygen	O_2	[mg/l]	Xylem Ysi	$\pm 0,1$mg/l	10Hz

Table 1: List over all sensors used during the experiment, their uncertainties and sampling rate.

3. Results and validation

The mean measured strain at $BS1$ is shown in Figure 5. Similar results were also seen in the results from $BS2$ and $BS3$, while $BS4$ had a failing connection or wire which caused it to drift out of the range of the measurement equipment. The standard deviation of the measured signal were in the range of $0,35\mu\epsilon$ to $2,3\mu\epsilon$ for all strain gauge measurements.

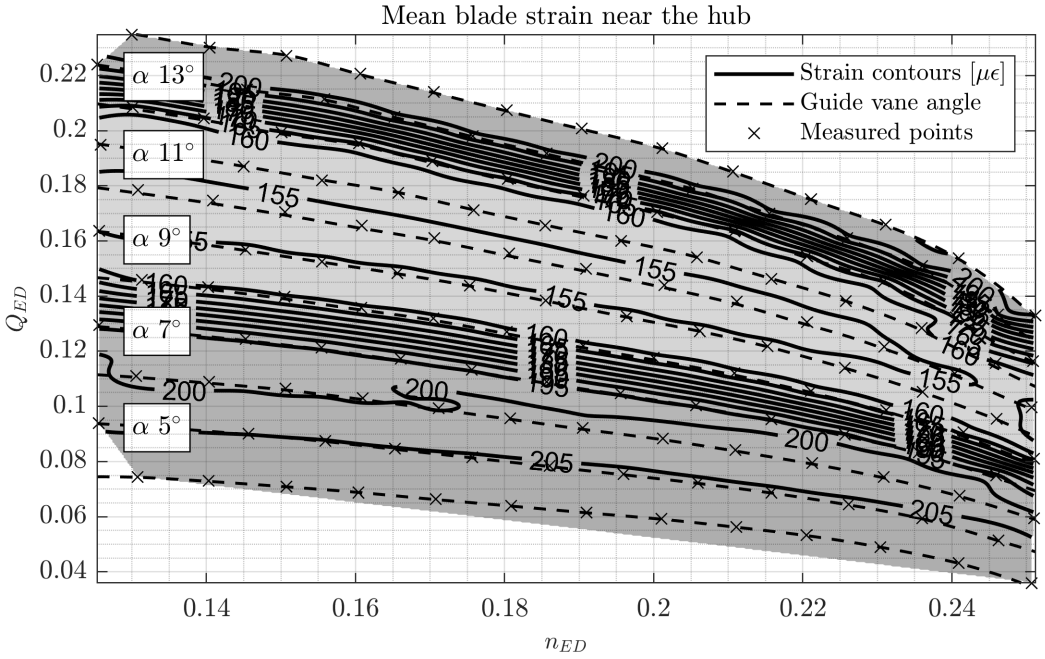

Figure 5: Contour of the measured mean blade strain near the hub ($BS1$).

In order to confirm the repeatability and validity of all the measurements through out the measurement campaign, one operating point was chosen as a reference point and repeatedly logged at the beginning and end of each day as well as in between measurement series. This point was set to be at n_{ED} of $0,18$, α of $10°$ and H_n of 12m. In total, thirteen reference point repetitions were measured in relation to the results presented in this paper. The strain gauge measurements for the reference points can be seen in Figure 6, note $BS4$'s deviation from the general trend. As a result of $BS4$'s deviation none of the results from that gauge were considered during the post processing.

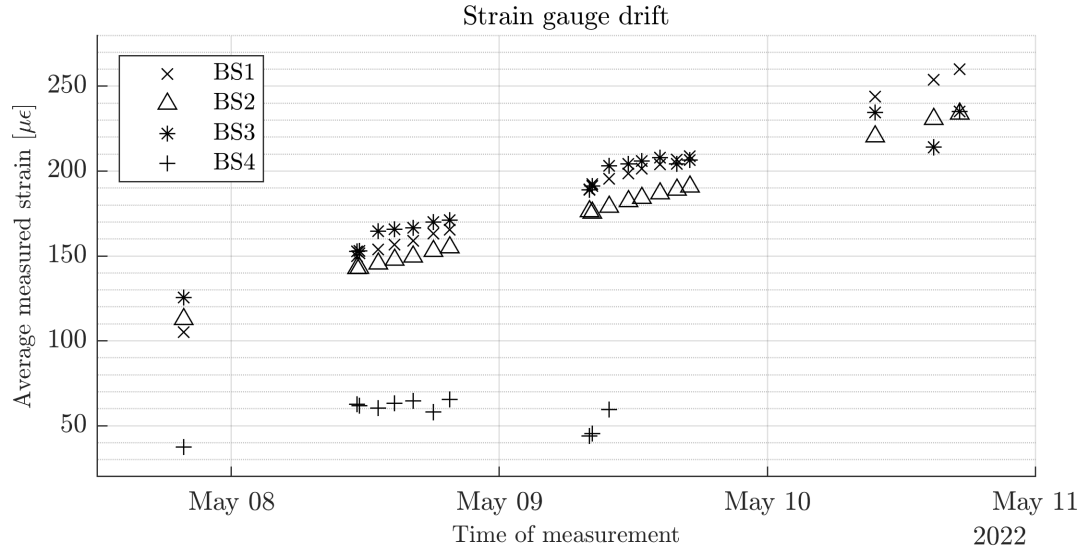

Figure 6: Measured drift over the course of the experiment at the reference point.

If the drift is sorted by which guide vane angle each reference was taken before instead of chronologically, illustrated in Figure 7, it becomes clearer how the drift skewed the data with the lowest mean strain at 10° opening as that was the first measurement series taken during the campaign.

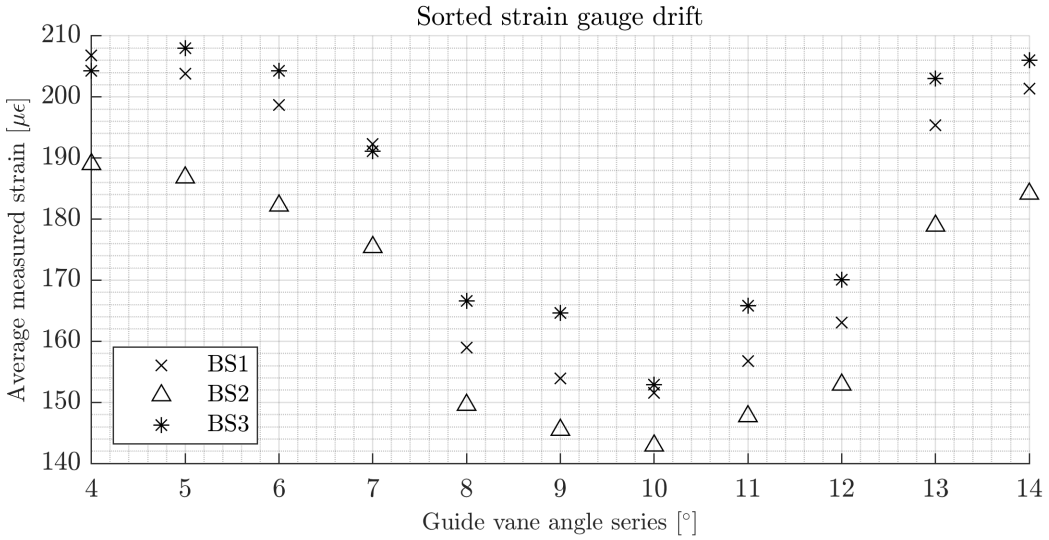

Figure 7: Measured drift sorted by which guide vane opening series each point preceded.

Figure 8 shows the results from adjusting for the drift of the strain gauges over the time of measurement. The adjustment is done by subtracting the mean strain with the drift measured at the repeated reference point, meaning that the values are no longer absolute but the difference between the measured strain and the mean strain at BEP for that point in time.

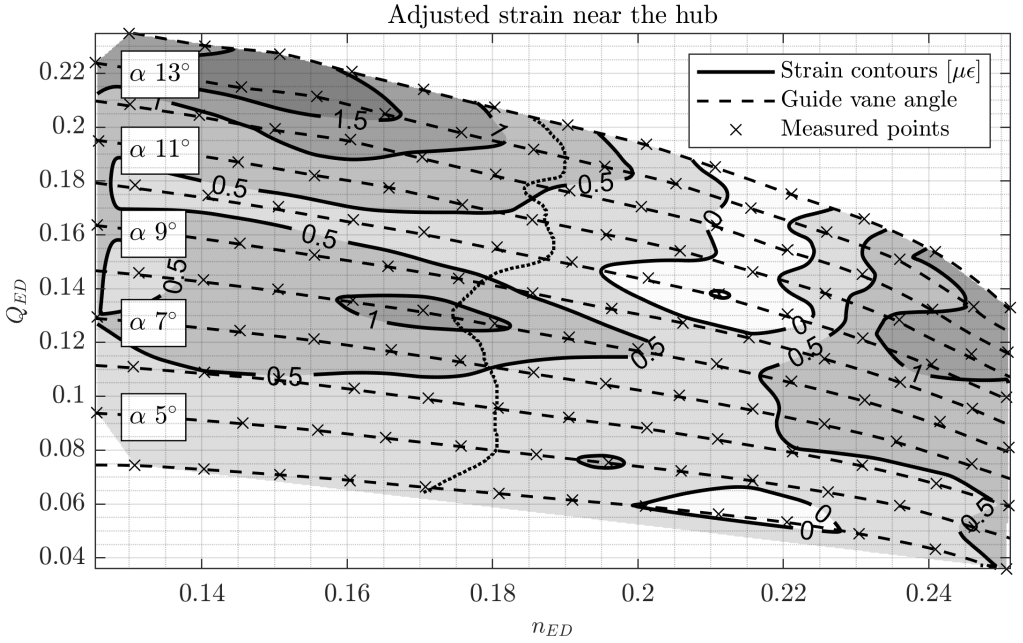

Figure 8: Contour of the apparent strain when compensating for the drift ($BS1$).

When compensating for the drift, there is no similarity between the measurements from $BS1 - BS3$. Some difference in the mean strain is to be expected between the gauges near the hub and shroud ($BS1$ & $BS2$), but similar trends would be expected when comparing two hub mounted gauges for instance ($BS1$ & $BS3$), as seen in Figure 9.

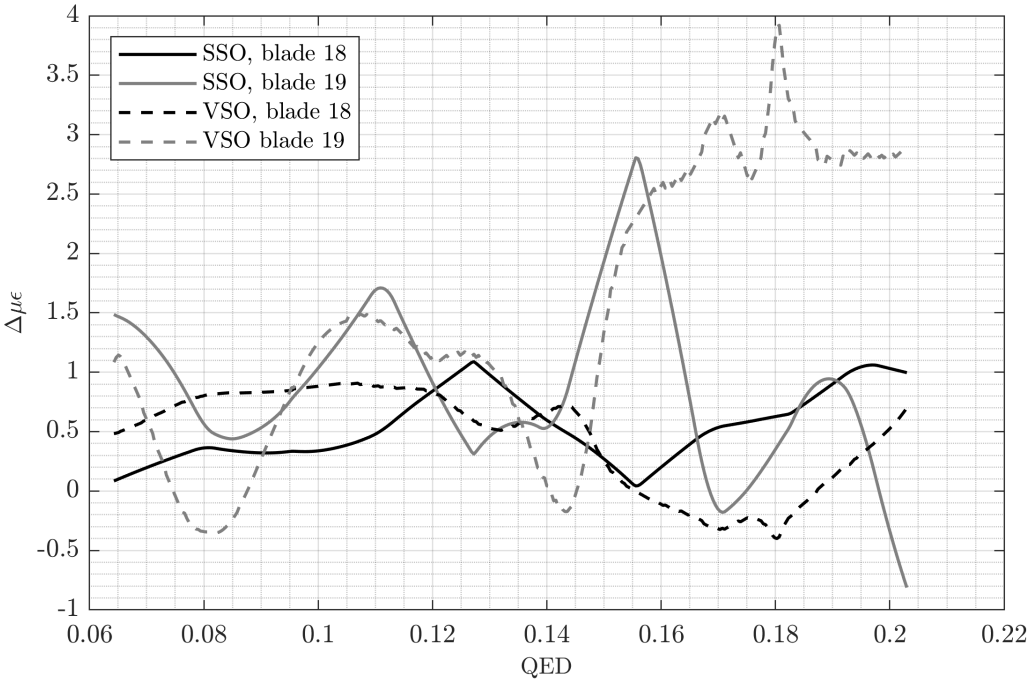

Figure 9: Comparing the strain measurements near the hub on both blades ($BS1$ & $BS3$)

SSO, or synchronous speed operation is taken at a fixed n_{ED} of $0,18$. VSO, or variable speed operation is an operation scheme which follows the line of highest hydraulic efficiency for any guide vane opening.

Table 2: Measured change in strain between unloaded and BEP load through out the campaign

Time between points	Strain difference		
	BS1	BS2	BS3
00:07:39	-0,59511	0,897605	-1,86688
00:05:46	-0,61241	0,673372	-1,83541
00:11:52	-1,59027	0,591596	-4,27784
00:08:44	-0,71338	0,576053	-3,98752
00:15:45	-1,17821	0,402121	-6,54958
00:05:59	-0,33918	0,942753	-5,8496

At the beginning and end of each day measurements were done while the runner was stationary and submerged as well as operating at BEP, so the static strain at BEP operation can be found by calculating the difference between BEP and stationary. The difference is presented in Table 2.

4. Discussion, conclusion and further work

4.1. Drift and systematic error

At first glance looking at Figure 5 it might seem like there is an increase in the mean strain on the runner blade when moving away from a guide vane opening of 10°. The contour lines also seem to almost perfectly follow the guide vane lines, i.e. not being dependent on the n_{ED} at all. This result however turned out to be an artefact caused by the order of which the measurements were performed, and the same trends could be seen from the reference measurement points taken throughout the campaign. With the recorded reference points, it was attempted to offset the measured values at each point with the corresponding reference data and see if there were any trends in the measured strain but since the mean strain at any point was unknown, the adjusted values is close to zero, and are almost one order of magnitude less than the standard deviation of the raw signal. The primary cause of the drift seen through the experiment is assumed to be a result of the water temperature slowly increasing, starting at $14,7$°C and reaching $16,5$°C by the end of the campaign. The increase in water temperature is suspected to be a result of both the water running through uninsulated pipes and tanks in a room with a higher air temperature than what the water had, and the mechanical losses in various parts of the system adding some extra heat.

4.2. Electrical noise

Another issue encountered during the measurement campaign was excessive noise on the amplified onboard signals. This noise would only appear when the generator was turned on, so the source is believed to be the alternating current in the machine and cables. The main frequencies seen in the noisy signals were harmonics of the frequency of the AC generator, and the observed level of noise in the signal increased by $3-4\times$ when the generator turned on.

4.3. Comparison with numerical simulation

Some preliminary structural simulations of the runner were performed early on in HydroFlex, and from those the expected strain at the locations of the gauges was extracted for operation at BEP. During the measurement campaign data was also recorded with the runner stationary but still submerged in water shortly after reference measurements at BEP, meaning that the difference in mean strain from stationary and BEP operation should be the absolute strain at BEP. However, this difference was an order of magnitude lower than what was seen in the simulations. The measurements were repeated multiple times throughout and there is a significant difference in between each of them, which would at least indicate that the experimental result is non conclusive.

4.4. Further work

The next step in this process now is to identify where in the measurement chain the noise is picked up, i.e. if it is from the cables running through the turbine shaft, before the amplification, or maybe even from the power source feeding the amplifiers. Secondly, more sensitive strain gauges are needed, as the mean value of the strain seems to be relatively unaffected by changing loads compared with the standard deviation of the signal. Finally, a better way to compensate for temperature related drift since there is no practical way to control the water temperature in the test rig at the Waterpower Laboratory. The compensation can either be by having some variability of one or more resistors in the Wheatstone bridge, or record the drift more frequently when the turbine runner is stationary but still submerged.

Acknowledgements
The work associated with this paper has been done under the HydroFlex project which received funding from the European Union's Horizon 2020 research and innovation programme under grant agreement No 764011. As a part of HydroFlex, the research on the mechanical and hydraulic aspects of turbines were conducted in work package 3 with the partners the Norwegian University of Science and Technology (NTNU), EDR Medeso, Rainpower, Ss. Cyril and Methodius University in Skopje, and Luleå University of Technology.

References

[1] European Commission. *A policy framework for climate and energy in the period from 2020 to 2030.* 2014.

[2] European Commission. *A clean planet for all. A European strategic long-term vision for a prosperous, modern, competitive and climate neutral economy.* 2018.

[3] International Electrotechnical Commission. *60193:2019 Hydraulic turbines, storage pumps and pump-turbines - Model acceptance tests.* 2019.

[4] Norwegian University of Science and Technology. *HydroFlex - Increasing the value of Hydropower through increased Flexibility.* URL: https://www.h2020hydroflex.eu/ (visited on 20/01/2023).

[5] Einar Kobro, Torbjørn Kristian Nielsen and Ole Gunnar Dahlhaug. 'Data analysis from onboard francis model runner pressure measurements'. In: *13th International Symposium on Transport Phenomena and Dynamics of Rotating Machinery 2010, ISROMAC-13.* 2010, pp. 98–103.

[6] Norwegian Hydropower Centre. *Francis-99.* URL: https://www.ntnu.edu/nvks/francis-99 (visited on 20/01/2023).

[7] Igor Iliev. *HydroFlex D3.4 - Hydraulic and mechanical design of the Francis model turbine.* Tech. rep. 2020.

[8] Norwegian University of Science and Technology. *HydroCen.* URL: https://www.ntnu.no/hydrocen (visited on 20/01/2023).

[9] Igor Iliev et al. 'Optimization of Francis Turbines for Variable Speed Operation Using Surrogate Modeling Approach'. In: *Journal of Fluids Engineering* 142.10 (Aug. 2020). 101214. ISSN: 0098-2202. DOI: 10.1115/1.4047675. eprint: https://asmedigitalcollection.asme.org/fluidsengineering/article-pdf/142/10/101214/6554501/fe_142_10_101214.pdf. URL: https://doi.org/10.1115/1.4047675.

[10] Hottinger Baldwin Messtechnik GmbH. *Strain Gauges - Absolute precision from HBM.* Datasheet. 2018. URL: https://pdf.directindustry.com/pdf/hbm-test-measurement/hbm-estrain-gauge-catalog/6017-266731.html#open614644 (visited on 20/01/2023).

[11] VPG Vishay Foil Resistors. *High precision foil resistor with TCR of* $\pm 2.0 ppm/^{\circ}C$*, tolerance of* $\pm 0.005\%$ *and load life stability of* $\pm 0.005\%$. Datasheet. 2015. URL: https://foilresistors.com/docs/63001/63001.pdf (visited on 26/01/2023).

[12] Mantracourt. *ICA emedded strain gauge analogue amplifiers.* 2018. URL: https://www.mantracourt.com/userfiles/documents/ica_user_manual.pdf (visited on 26/01/2023).